Multiple circadian transcriptional elements cooperatively regulate cell-autonomous transcriptional oscillation of *Period3*, a mammalian clock gene

Received for publication, July 14, 2017, and in revised form, August 7, 2017 Published, Papers in Press, August 15, 2017, DOI 10.1074/jbc.M117.806836

Ritsuko Matsumura and Makoto Akashi[1]

From the Research Institute for Time Studies, Yamaguchi University, 1677-1 Yoshida, Yamaguchi 753-8511, Japan

Edited by Ronald C. Wek

Cell-autonomous oscillation in clock gene expression drives circadian rhythms. The development of comprehensive analytical techniques, such as bioinformatics and ChIP-sequencing, has enabled the genome-wide identification of potential circadian transcriptional elements that regulate the transcriptional oscillation of clock genes. However, detailed analyses using traditional biochemical and molecular-biological approaches, such as binding and reporter assays, are still necessary to determine whether these potential circadian transcriptional elements are actually functional and how significantly they contribute to driving transcriptional oscillation. Here, we focused on the molecular mechanism of transcriptional oscillations in the mammalian clock gene *Period3* (*Per3*). The PER3 protein is essential for robust peripheral clocks and is a key component in circadian output processes. We found three E box–like elements located upstream of human *Per3* transcription start sites that additively contributed to cell-autonomous transcriptional oscillation. However, we also found that *Per3* is still expressed in a circadian manner when all three E box–like elements are functionally impaired. We noted that *Per3* transcription was activated by the synergistic actions of two D box–like elements and the three E box–like elements, leading to a drastic increase in circadian amplitude. Interestingly, circadian expression of *Per3* was completely disrupted only when all five transcriptional elements were functionally impaired. These results indicate that three E box–like and two D box–like elements cooperatively and redundantly regulate cell-autonomous transcriptional oscillation of *Per3*.

Almost all organisms exhibit circadian rhythms in physiology and behavior, which are driven by the circadian clock. The circadian clock enables maximum expression of genes at appropriate times of the day, allowing organisms to adapt to the earth's rotation. The circadian clock is phase-adjusted in response to environmental cues such as light and nutrients in a flexible but phase-dependent manner. The suprachiasmatic nucleus functions as a standard clock and orchestrates peripheral clocks to prevent internal desynchronization (1). The molecular machinery for the circadian clock is cell-autonomous and ubiquitous throughout the body (2, 3). The circadian clockwork consists of a negative feedback loop of transcription, which drives circadian gene expression (4). In mammals, the BMAL1 and CLOCK complex activates transcription of clock and clock-related genes, such as *Period* (*Per*) and *Cryptochrome* (*Cry*) via E-box elements. Subsequently, PER together with CRY, a potent transcriptional inhibitor, function to negatively regulate this complex (5, 6). Recent studies have suggested that the PER-mediated transient neutralization of CRY may cause a time delay in CRY-mediated transcriptional repression, which may help to extend the transcriptional oscillation period (7–9).

The mammalian clock gene, *Period3* (*Per3*), one of three homologs of the *Drosophila* gene, *Period*, was cloned in 1998 (10, 11). Studies have shown that the circadian period length of locomotor activity rhythms in *Per3*-deficient mice are ~0.5 h shorter than that in wild-type mice, whereas other circadian characteristics examined are mostly normal compared with mice lacking *Per1* and *Per2* (12, 13). Therefore, it has been hypothesized that PER3 protein has a dispensable role in the clock oscillator machinery. However, recent studies indicate that PER3 protein may be a tissue-specific component of peripheral clocks (14, 15). In addition, genetic analyses of human sleep disorders have revealed that circadian rhythm sleep disorders, such as delayed sleep phase syndrome, are associated with polymorphisms in the coding region of *Per3* (16, 17), suggesting that PER3 may contribute to circadian physiological and behavioral outputs. Furthermore, recent studies indicate that *Per3* polymorphisms with amino acid changes are associated with familial advanced sleep phase accompanied with mood disorders (18). Additionally, PER3 protein may be an inhibitor of adipocyte cell fate, because *Per3*-deficient mice have greater adiposity compared with wild-type mice (19). Therefore, better molecular understanding of PER3 function would benefit further research into the prevention and treatment of these circadian-related disorders.

Because cell-autonomous oscillation in clock gene expression is the central machinery that drives circadian rhythms in physiology and behavior, deciphering the molecular mechanisms of the transcriptional oscillation of *Per3* will contribute to the general understanding of the circadian system. Although a few studies have examined parts of this mechanism using comprehensive analytical approaches, there is currently no consensus on the mechanism underlying *Per3* transcriptional oscillation. For example, *Bmal1*-deficient mice show drastically reduced circadian amplitude of *Per3* expression, indicating an

This work was supported by a grant-in-aid for scientific research (KAKENHI). The authors declare that they have no conflicts of interest with the contents of this article.

[1] To whom correspondence should be addressed. E-mail: akashima@yamaguchi-u.ac.jp.

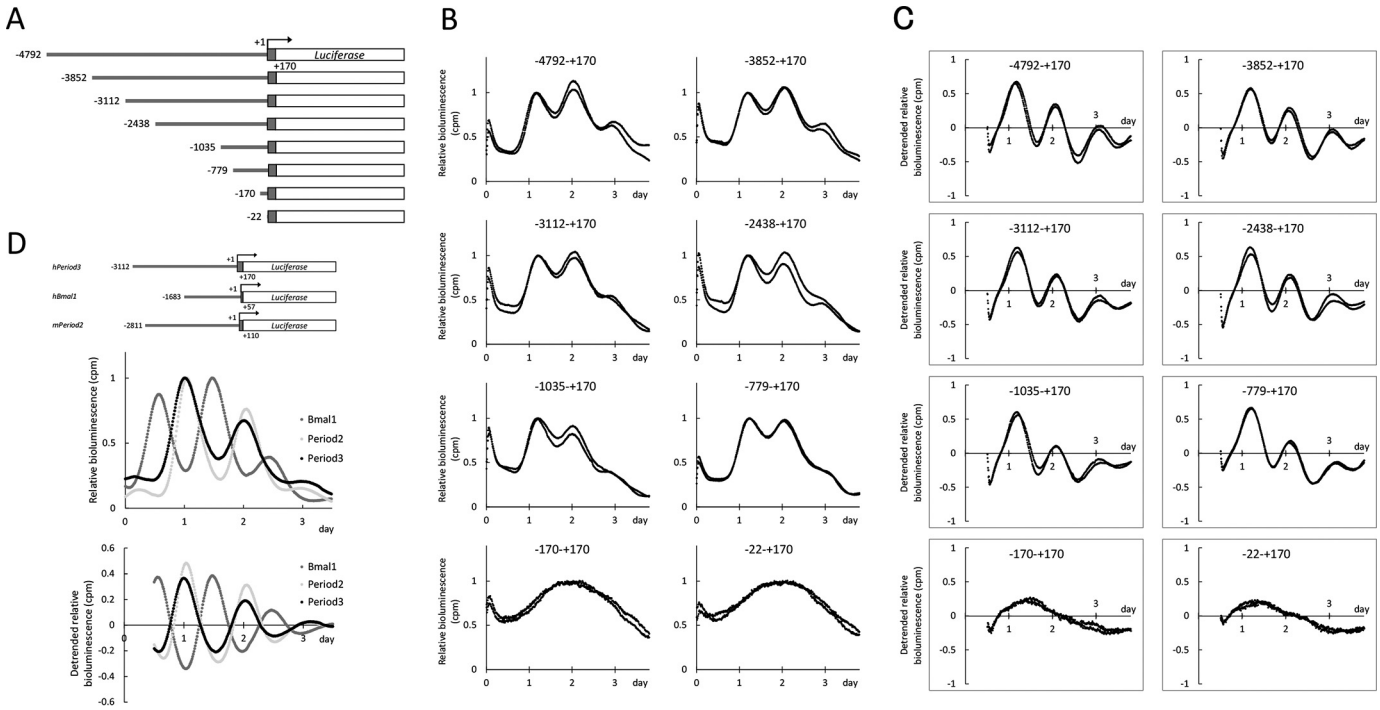

Figure 1. Mapping of the region responsible for the transcriptional oscillation of *Per3*. *A*, schematic representation of the luciferase reporter gene constructs generated by deleting sequences throughout the *Per3* transcription-regulatory region. *+1* corresponds to the transcription start site. *B*, transcriptional oscillation of *Per3* monitored in U2OS cells transfected with the *hPer3-luc* constructs indicated in *A*. After synchronization by dexamethasone treatment (50 nM for 2 h), bioluminescence was measured in the presence of luciferin and integrated for 1 min at 15-min intervals. The peak value of the first curve was set to 1. Relative bioluminescence (*y* axis) was measured in cpm. The data are from two independent experiments. *C*, detrended oscillation curves of the data sets in *B* obtained by subtracting the 24-h simple moving average from the respective raw data. *D*, circadian transcriptional oscillation of clock genes, *hBmal1*, *mPer2*, and *hPer3*, in U2OS cells transfected with the adenovirus reporter vectors indicated in the *top panel*. After synchronization by dexamethasone treatment (50 nM for 2 h), bioluminescence was measured in the presence of luciferin and integrated for 1 min at 15-min intervals. Maximum peak values were set to 1. The acrophase was calculated using cosine curve-fitting analysis and compared among the three clock genes. Data were from a single assay.

indispensable role of E box-mediated regulation in *Per3* transcriptional oscillation (20). In support of this result, a ChIP-seq analysis using antibodies targeting circadian transcription factors showed their binding to the upstream region of *Per3* transcription start sites (21). However, the specific location of the binding sites and the functional significance of this binding remain unclear. In contrast, a study that combined bioinformatics with experimental validations reported that transcriptional oscillation of the *Per3* gene may be regulated by two D-box transcriptional elements (22). However, it remains unclear whether or not functional impairment of these transcriptional elements impairs *Per3* circadian transcription.

To clarify the mechanism by which the *Per3* gene is expressed in a cell-autonomous circadian manner, we investigated whether individual potential circadian transcriptional elements were actually functional for cell-autonomous circadian transcription using traditional biochemical and molecular-biological approaches.

Results

The −779 to −170 transcription-regulatory region is essential for the cell-autonomous circadian transcription of Per3

Because various extracellular factors can affect clock gene expression *in vivo*, real-time monitoring of clock-driven bioluminescence in culture is a powerful method for investigating the molecular mechanisms underlying cell-autonomous circadian transcription.

To narrow down the genomic region essential for cell-autonomous circadian transcription of *Per3*, deletion constructs of *Per3* (−4792 to +170) −*luciferase* (*luc*) were generated using restriction enzymes (Fig. 1*A*) and transfected into U2OS cells. Under culture conditions, individual cellular clocks are probably desynchronized from each other due to the absence of suprachiasmatic nucleus–driven orchestration (23), resulting in a low amplitude of transcriptional rhythms at the cell-population level. Dexamethasone (DEX),[2] which transiently activates the clock gene *Period1* via glucocorticoid receptors, is a well-known synchronizer for peripheral clocks (24). Therefore, after synchronization of cellular clocks by DEX treatment, real-time and continuous monitoring of bioluminescence was performed for a few days (Fig. 1*B*). Comparisons among the six constructs from *Per3* (−4792 to +170) to *Per3* (−779 to +170) revealed clear circadian rhythms of bioluminescence in all cases, although a deletion-induced minor decrease in circadian amplitude was observed. In contrast, cells containing *Per3* (−170 to +170) −*luc* and *Per3* (−22 to +170) −*luc* showed no obvious circadian rhythms in bioluminescence. These circadian rhythmicity evaluations were further assessed using detrended data, which were generated by subtracting the 24-h moving average from the raw data. Cosine curve fitting for detrended data demonstrated a significant circadian oscillation

[2] The abbreviations used are: DEX, dexamethasone; E′1, E′2, and E′3, E′ box 1, 2, and 3, respectively; DBP, albumin D-box–binding protein.

in cells containing the six constructs from *Per3* (−4792 to +170) to *Per3* (−779 to +170). In contrast, analysis of detrended data confirmed that circadian rhythms were not detectable in cells containing *Per3* (−170 to +170) −*luc* and *Per3* (−22 to +170) −*luc* (Fig. 1*C*). These results clearly suggest that the genomic region, *Per3* (−779 to −170), plays a pivotal role in the cell-autonomous circadian transcription of *Per3*.

We also examined whether *Per3*-driven bioluminescence rhythms accurately reflect the expression characteristics of endogenous *Per3*. U2OS cells were infected with adenovirus vectors containing *Per3-*, *Per2-*, or *Bmal1-luc*, and after synchronization by DEX treatment, real-time and continuous monitoring of bioluminescence was performed for a few days (Fig. 1*D*). Previous studies have shown that the circadian phase of endogenous *Per2* mRNA levels is slightly delayed compared with that of *Per3*, whereas endogenous *Bmal1* mRNA levels are antiphasic to that of *Per2* and *Per3* (25). The circadian phase relationship among these three genes was highly consistent between endogenous mRNA and bioluminescence levels. We compared the phase intervals of bioluminescence rhythms obtained using three adenovirus vectors in this study with those of endogenous mRNA rhythms reported previously (25); the phase intervals of bioluminescence and endogenous mRNA rhythms between *Bmal1* and *Per3* were 12.1 and 12.2 h, whereas those between *Bmal1* and *Per2* were 13.2 and 13.3 h, respectively. This result strongly suggests that the genomic region used in this study contains almost all endogenous transcriptional elements essential for cell-autonomous circadian transcription of *Per3*.

Three E box–like transcriptional elements cooperatively regulate the cell-autonomous circadian transcription of Per3

An *in silico* search revealed that the *Per3* (−779 to −170) region contains three E box–like sequences (in order from upstream to downstream): E′ box 1 (E′1, CACGCG), E′ box 2 (E′2, CACGCG), and E′ box 3 (E′3, CTCGAG) (Fig. 2*A*). Previous studies indicate that the circadian transcription factors BMAL1 and CLOCK bind to canonical E box (CACGTG) as a heterodimer to activate transcription (26). A comprehensive ChIP-seq analysis revealed that BMAL1 binds around −335 upstream of the transcription start site of *Per3* (21), which corresponds to the location of the three E′-boxes within the region −445 to −389. To determine whether BMAL1 and CLOCK activate these three E′-boxes, we performed a reporter assay (Fig. 2*B*) using various deletion mutants of the *Per3* (−779 to +170) region, as schematically shown in Fig. 2*A*. BMAL1-CLOCK-mediated transcriptional activation was reduced by the loss of E′1 and E′3 but not E′2. As expected, double-deletion mutants, such as Δ(E′1, E′2) and Δ(E′1, E′3), exhibited further reduced transcriptional activity compared with single-deletion mutants. Unexpectedly, however, the double deletion mutant Δ(E′2, E′3) showed increased transcriptional activity compared with the single deletion mutant ΔE′3. In the absence of all three E′-boxes, BMAL1 and CLOCK could no longer activate transcription. These results demonstrate that the three E′-boxes function as circadian transcriptional elements in an independent and cooperative manner.

The physical interaction between BMAL1-CLOCK and E′-boxes was examined by an EMSA (Fig. 2*C*). Incubation of affinity-purified Myc-tagged BMAL1 and FLAG-tagged CLOCK with a ^{32}P-labeled DNA probe containing E′1 resulted in an expected mobility-shifted band containing a complex of proteins and DNA by electrophoresis. This band was abolished by the addition of an excess amount of a non-labeled competitor. Co-incubation of anti-Myc or FLAG antibody induced a supershifted band, confirming specific binding. No mobility-shifted band was detected when using a probe containing nucleotide-substituted E′1. Interestingly, whereas no shifted band was detected using probes containing E′2 or E′3 alone, both a shifted and supershifted band were observed when using a probe containing both E′2 and E′3. This suggests that BMAL1 and CLOCK bind to tandemly arranged E′2 and E′3 in an interdependent manner.

To investigate whether the E′ boxes are indispensable for the cell-autonomous circadian transcription of *Per3*, real-time and continuous monitoring of bioluminescence was performed in cells transfected with a construct lacking E′ boxes in the transcription-regulatory region in various combinations (Fig. 2*D*). Whereas ΔE′1 and ΔE′3 showed reduced *Per3* expression levels, ΔE′2 showed unexpected enhanced expression and a shallow circadian trough, indicating the action of a transcription repressor on E′2 that is independent of E′3. When E′3 is dysfunctional, we hypothesize that whereas BMAL1-CLOCK cannot bind to E′2, this transcription repressor can; for example, whereas BMAL1-CLOCK activates neither the Δ(E′1, E′2) nor Δ(E′1, E′3) construct, the transcription repressor can regulate the latter, leading to differing expression levels of the two constructs. This hypothetical transcription repressor may also explain the higher transcriptional activity arising from the Δ(E′2, E′3) construct compared with ΔE′3 (Fig. 2, *B* and *D*). Detrended data more clearly demonstrate the reduced transcriptional amplitude in ΔE′1 and ΔE′3 and the shallow trough in ΔE′2 (Fig. 2*E*). The interdependency of E′2 and E′3 in transcriptional activation and the independency of E′2 in transcriptional repression can explain all phenotypic outputs observed using constructs lacking E′ boxes in various combinations. For example, whereas both the Δ(E′1, E′2) and Δ(E′1, E′3) constructs exhibited low amplitude transcription because they were not activated by BMAL1-CLOCK, the latter exhibited a deeper circadian trough via the circadian action of a transcription repressor on E′2, leading to differing circadian robustness between these constructs. Importantly, circadian rhythms in bioluminescence remained detectable even in the absence of all three E′ boxes, strongly suggesting the action of other circadian transcriptional elements.

Cosine curve fitting was performed using detrended data to calculate circadian robustness, amplitude, and phase (Fig. 2, *F–H*). Although circadian robustness was over 75% for all constructs, it was significantly lower for constructs lacking functional E′2 compared with the others due to the shallow circadian trough. Circadian amplitude was reduced in ΔE′1 and ΔE′3 but not ΔE′2 constructs. Differences in amplitude among double deletion mutants may be explained by the hypothesis that neither circadian transcription factors nor repressor(s) can bind to Δ(E′1, E′2), only circadian transcription repressor(s)

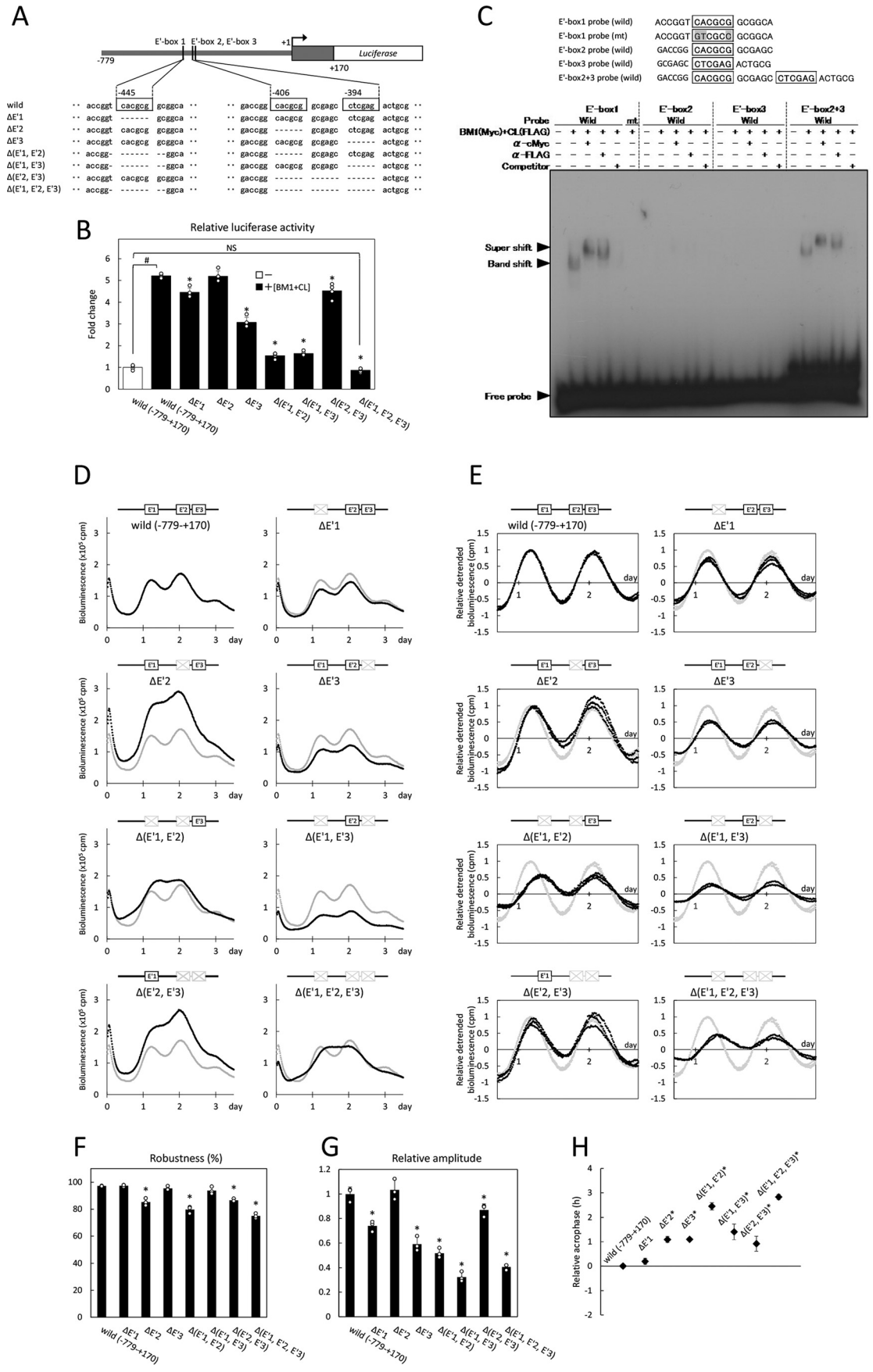
A
E'-box 1 E'-box 2, E'-box 3
+1
Luciferase
-779
+170
-445
-406
-394
wild
ΔE'1
ΔE'2
ΔE'3
Δ(E'1, E'2)
Δ(E'1, E'3)
Δ(E'2, E'3)
Δ(E'1, E'2, E'3)
B
Relative luciferase activity
NS
#
□ −
■ +[BM1+CL]
Fold change
wild (-779-+170)
ΔE'1
ΔE'2
ΔE'3
Δ(E'1, E'2)
Δ(E'1, E'3)
Δ(E'2, E'3)
Δ(E'1, E'2, E'3)
C
E'-box1 probe (wild) ACCGGT CACGCG GCGGCA
E'-box1 probe (mt) ACCGGT GTCGCG GCGGCA
E'-box2 probe (wild) GACCGG CACGCG GCGAGC
E'-box3 probe (wild) GCGAGC CTCGAG ACTGCG
E'-box2+3 probe (wild) GACCGG CACGCG GCGAGC CTCGAG ACTGCG
Probe
BM1(Myc)+CL(FLAG)
α−cMyc
α−FLAG
Competitor
Super shift
Band shift
Free probe
D
wild (-779-+170)
ΔE'1
ΔE'2
ΔE'3
Δ(E'1, E'2)
Δ(E'1, E'3)
Δ(E'2, E'3)
Δ(E'1, E'2, E'3)
Bioluminescence (x10⁵ cpm)
day
E
Relative detrended bioluminescence (cpm)
day
F
Robustness (%)
G
Relative amplitude
H
Relative acrophase (h)
wild (-779-+170)
ΔE'1
ΔE'2*
ΔE'3*
Δ(E'1, E'2)*
Δ(E'1, E'3)*
Δ(E'2, E'3)*
Δ(E'1, E'2, E'3)*

can bind to Δ(E′1, E′3), and only circadian transcription factors can bind to Δ(E′2, E′3). The difference in amplitude correlates with the results of our reporter assay experiments (Fig. 2*B*). Circadian phase for all deletion constructs, except ΔE′1, was significantly delayed compared with wild type. The constructs lacking all functional E′ boxes, Δ(E′1, E′2) and Δ(E′1, E′2, E′3), exhibited delays of >2 h. This phase delay may be due to the presence of other types of circadian transcriptional elements, because deletion of E′ boxes in the case that circadian transcription of *Per3* is controlled by only E box–type elements should result in a reduced amplitude but not a phase shift. Although our results from reporter assays shown in Fig. 2*B* suggest the absence of other BMAL1-CLOCK–responsive elements in the *Per3* region (−779 to +170) apart from the three E′ boxes, circadian rhythms in bioluminescence remained detectable when all three E′ boxes were deleted, supporting the hypothesis that other types of circadian transcriptional elements are present.

Two D box–like transcriptional elements regulate the cell-autonomous circadian transcription of Per3

An *in silico* analysis identified two D box–like sequences within the *Per3* region −779 to −170 (Fig. 3*A*): a canonical D box (−589, TTATGTAA) and a non-canonical D′ box (−548, TTATATAA). Although a previous report demonstrated that these D box–like sequences can regulate the *SV40* promoter in a circadian manner (22), it remains unknown whether they are actually required for cell-autonomous circadian transcription of *Per3*. To examine this, we generated *Per3* (−779 to +170) constructs lacking these two sites and examined their function using reporter assays (Fig. 3*B*). Overexpression of DBP induced minor (~2-fold) activation of *Per3*. Deletion of either of the D/D′ boxes resulted in similar or reduced transcriptional activation, whereas deletion of both D/D′ boxes completely abolished DBP-induced activation. Interestingly, overexpression of BMAL and CLOCK elevated DBP-mediated activation by >9-fold, suggesting their synergistic cooperation in regulating *Per3* transcription.

We examined the contribution of the D/D′ boxes to the circadian transcription of *Per3* (Fig. 3*C*). Deletion of either of the D/D′ boxes resulted in reduced expression of *Per3*. The contribution of the D′ box to expression levels was higher than that of the D box. Circadian rhythms in bioluminescence remained detectable in the absence of both D/D′ boxes. Detrended data highlighted the contribution of the D/D′ boxes to circadian amplitude and revealed changes in the circadian phase in deletion mutants (Fig. 3*D*). To evaluate the effect of D/D′-box deletions on circadian characteristics in detail, cosine curve fitting was performed using detrended data to calculate circadian robustness, amplitude, and phase (Fig. 3, *E*–*G*). Interestingly, whereas deletion of the D/D′ boxes resulted in a drastic reduction in amplitude, circadian robustness remained close to 100%, indicating that the D/D′ boxes contribute to increasing amplitude rather than driving oscillation. Loss of either or both of the D/D′ boxes advanced the circadian phase of *Per3* transcription, an opposing phenotype to that observed after the deletion of E′ boxes (Fig. 2*H*).

Three E′ boxes and two D/D′ boxes cooperatively control the cell-autonomous circadian transcription of Per3

Because the separate deletion of either all E′ boxes or all D/D′ boxes did not completely abolish the circadian transcription of *Per3*, we examined the effect of simultaneously deleting all three E′ boxes and two D/D′ boxes on circadian transcription (Fig. 4*A*). We constructed a total of 20 reporter vectors by introducing single or double deletions of D/D′ boxes into the *Per3* (−779 to +170) region lacking E′ boxes in different combinations. Our data clearly demonstrate the contribution of the D/D′ boxes to *Per3* expression levels. Importantly, deletion of the D/D′ boxes in the absence of all three E′ boxes did not affect *Per3* expression levels. This indicates that D/D′ box–mediated transcriptional activation requires functional E′ boxes, which is consistent with our data showing that simultaneous overexpression of DBP and BMAL1-CLOCK results in the synergistic activation of *Per3* transcription. Detrended data clearly demonstrated that deletion of the D/D′ boxes decreased the amplitude

Figure 2. Effects of the E′-box element on the circadian transcriptional oscillation of *Per3*. *A*, schematic representation of the *hPer3-luc* constructs including surrounding nucleotide sequences of the targeted E′ boxes selected from an *in silico* search. *+1* corresponds to the transcription start site. *Square boxes* and *dashes* indicate the targeted E′-box elements and deleted nucleotides, respectively. *B*, luciferase reporter assay investigating the effects of E′-box deletion on transcriptional activation by BMAL1 (BM1) and CLOCK (CL) proteins. U2OS cells cultured in a 24-well plate transfected with the indicated combination of vectors (a *hPer3-luc* reporter vector; *Renilla* luciferase vector, used as an internal control; and clock protein expression vectors). -Fold activation was normalized relative to luciferase activity of wild-type (−779 to +170) constructs in the absence of BM1 and CL as a control. Each value represents the mean ± S.D. (*error bars*) from four replicates of a single assay. *White circles* indicate individual data points from replicates. Mean values were compared with that of wild-type (−779 to +170) constructs containing BM + CL as controls using Dunnett's test, and *asterisks* indicate statistical significance ($p < 0.05$). A *t* test at $\alpha = 0.05$ was performed for two combinations: wild type (−779 to +170) *versus* wild type (−779 to +170) + [BM1 + CL] or wild type (−779 to +170) *versus* Δ (E′1, E′2, E′3) + [BM1 + CL], which are indicated by the *short* and *long brackets*, respectively. # and NS, statistical significance and no statistical significance, respectively. *C*, electrophoretic mobility shift assay. A ^{32}P-labeled double-stranded oligonucleotide containing the E′-box sequence(s) indicated in the *top panel* was used as a probe. Non-radiolabeled E′-box consensus probes were used as competitors. The *boxed* and *shaded* nucleotide sequences indicate the targeted E′-box and mutated nucleotides, respectively. Heterodimerized protein of Myc-BM1 and FLAG-CL were purified by immunoprecipitation using FLAG antibody–conjugated beads from HEK293A cells co-transfected with Myc-BM1 and FLAG-CL expression vectors. The BM1 + CL-bound probes are indicated by the *arrowhead labeled Band shift*. The addition of c-Myc or FLAG antibodies resulted in supershifted BM1 + CL-bound probes. Probes not bound to the proteins appeared as free probe. *D*, real-time monitoring of bioluminescence in U2OS cells transfected with the E′ box–deleted constructs indicated in *A*. Graphs show representative results from three replicates of a single assay. After synchronization by dexamethasone treatment (50 nM for 2 h), bioluminescence was measured in the presence of luciferin and integrated for 1 min at 15-min intervals. Bioluminescence (*y* axis) was measured in cpm. Schematic representations of the deleted E′-box elements (*light gray cross-marked boxes*) are indicated *above* each graph. *Light gray curves* represent the wild-type (−779 to +170) construct. *E*, relative detrended data sets obtained across a 2-day period were obtained by subtracting the 24-h simple moving average from three replicates of raw data. *Light gray curves* represent the wild-type (−779 to +170) construct, and the peak value of the first curve was set to 1. *F*–*H*, robustness, amplitude, and acrophase were calculated from the data set in *E* by curve fitting using the Cosinor software provided by Dr. Refinetti. The amplitude and acrophase of the wild-type (−779 to +170) construct were set to 1 and 0, respectively. The data indicate mean ± S.D. ($n = 3$). *White circles* in *F* and *G* indicate individual data points from replicates. The mean of each factor was compared with that of the wild type (−779 to +170) using the Dunnett's test, and *asterisks* indicate statistical significance ($p < 0.05$).

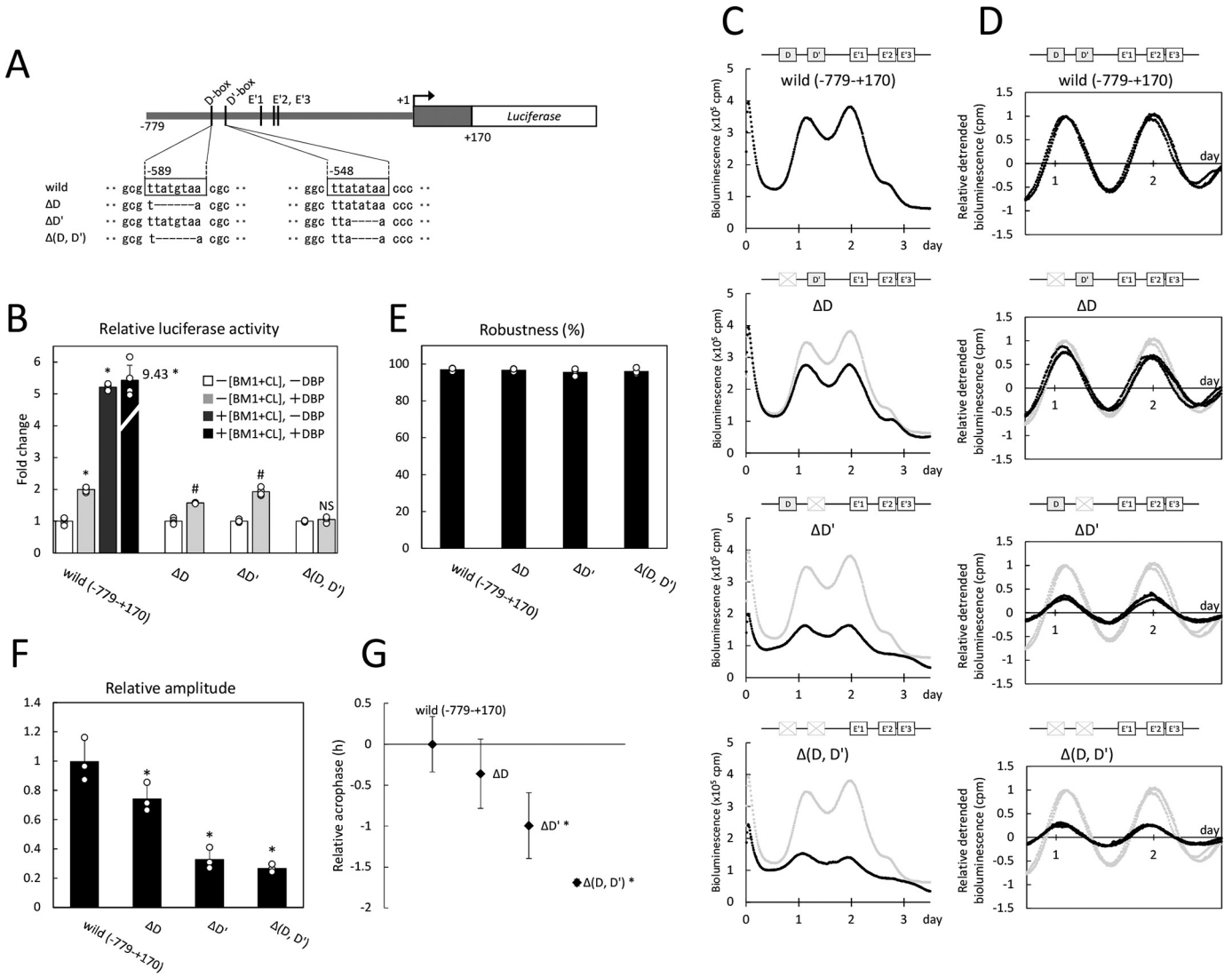

Figure 3. Effects of the D/D′-box element on the circadian transcriptional oscillation of *Per3*. *A*, schematic representation of the *hPer3-luc* constructs and deleted nucleotide sequences of the D/D′ boxes. *+1* corresponds to the transcription start site. *Square boxes* and *dashes* indicate the targeted D/D′-box elements and deleted nucleotides, respectively. *B*, luciferase reporter assay investigating the effects of D/D′-box deletion on transcriptional activation by DBP. U2OS cells cultured in a 24-well plate transfected with the indicated combination of vectors (a *hPer3-luc* reporter vector; *Renilla* luciferase vector, used as an internal control; and clock protein expression vectors). -Fold activation was normalized to luciferase activity in the absence of DBP (and BM1 + CL). Data indicate the mean ± S.D. (*error bars*) of four replicates from a single assay. *White circles* indicate individual data points from replicates. Among cells containing the wild-type (−779 to +170) construct, Dunnett's test ($\alpha = 0.05$) was used to analyze differences in mean values compared with the control, which contained no transcription factor (*white bar*), and *asterisks* indicate statistical significance ($p < 0.05$). # and *NS*, statistically significant and not significant differences determined by the *t* test at $\alpha = 0.05$ compared with controls (*white bars*), respectively. *C*, real-time monitoring of bioluminescence in U2OS cells transfected with the D/D′ box–deleted constructs indicated in *A*. Representative curves indicate data of three replicates from a single assay. After synchronization by dexamethasone treatment (50 nM for 2 h), bioluminescence was measured in the presence of luciferin and integrated for 1 min at 15-min intervals. Bioluminescence (*y* axis) was measured in cpm. Schematic representation of the deleted D/D′-box elements (*light gray cross-marked boxes*) are indicated *above* each graph. *Light gray curves* represent the wild-type (−779 to +170) construct. *D*, relative detrended data sets obtained across a 2-day period were obtained by subtracting the 24-h simple moving average from three replicates of raw data. The *light gray curves* represent the wild-type (−779 to +170) construct, and the peak value of the first curve was set to 1. *E–G*, robustness, amplitude, and acrophase from the data set in *D* were calculated by curve fitting using the Cosinor software provided by Dr. Refinetti. Amplitude and acrophase of the wild-type (−779 to +170) construct were set to 1 and 0, respectively. Data indicate the mean ± S.D. of three replicates, and *white circles* in *E* and *F* indicate individual data points from replicates. Mean values were compared with that of the control using the Dunnett's test, and *asterisks* indicate statistical significance ($p < 0.05$).

of *Per3* transcription and that circadian rhythms were almost completely abolished in Δ(D, D′, E′2), Δ(D, D′, E′3), Δ(D, D′, E′2, E′3), and Δ(D, D′, E′1, E′2, E′3) (Fig. 4*B*).

Cosinor analysis using detrended data revealed that deletion of the D/D′ boxes had no effect in ΔE′1 but significantly reduced circadian robustness in ΔE′3 (Fig. 4*C*). Deletion of E′2 led to relatively low robustness due to a shallow circadian trough, as already shown in Fig. 2 (*E* and *F*), and additional deletion of the D/D′ boxes further decreased robustness. Multiple deletion constructs, such as Δ(D, D′, E′2), Δ(D, D′, E′2, E′3), and Δ(D, D′, E′1, E′2, E′3), reduced robustness to less than 50%. Δ(D, D′, E′2, E′3) and Δ(D, D′, E′1, E′2, E′3) were classified as arrhythmic, as they showed non-circadian periods of *Per3* transcription (34 h or more) in two of three or all measurements, respectively. Although the negative effect of D/D′-box deletion on circadian amplitude was very strong, the effect in

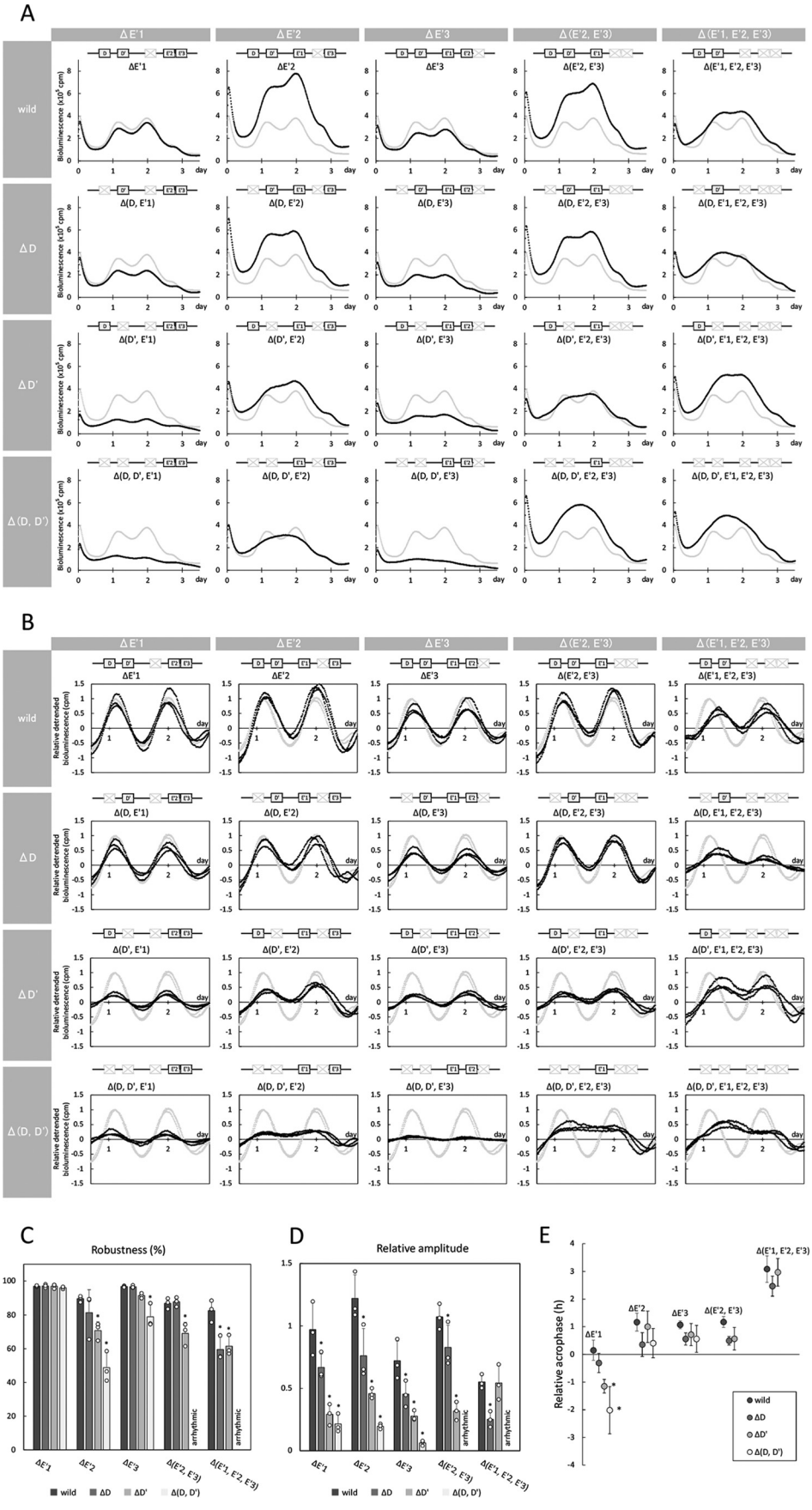
A
B
C
Robustness (%)
D
Relative amplitude
E
Relative acrophase (h)
wild
ΔD
ΔD'
Δ(D, D')
ΔE'1
ΔE'2
ΔE'3
Δ(E'2, E'3)
Δ(E'1, E'2, E'3)
arrhythmic
Bioluminescence (x10³ cpm)
Relative detrended bioluminescence (cpm)
day

the absence of all three E′ boxes was small or unclear due to the lack of DBP-mediated transcriptional activation (Fig. 4*D*). Consistent with the results in Fig. 3*G*, additional deletion of the D/D′ boxes in E′-box mutants resulted in a phase advance, which was statistically significant only for ΔE′1 constructs (Fig. 4*E*). The lack of statistically significant differences in phase may be attributed to the reduced reliability of the calculated phases in E′-box mutants due to the low robustness observed for all ΔE′ constructs except for ΔE′1 after the additional deletion of D/D′ boxes (Fig. 4*C*).

Discussion

Although PER3 is a component of peripheral clocks and has indispensable roles in circadian outputs, the mechanism underlying the cell-autonomous circadian transcription of *Per3* remains unclear. To elucidate this mechanism, we conducted detailed analyses of circadian transcriptional elements. The transcription-regulatory region examined in this study, *Per3* (−4792 to +170), contains almost all of the circadian transcriptional elements required for cell-autonomous circadian transcription of *Per3*. Although we focused on and further analyzed the core region *Per3* (−779 to −170), comparison of *Per3* (−4792 to +170) and *Per3* (−779 to +170) constructs (Fig. 1, *B* and *C*) showed that removal of a genomic region upstream of *Per3* (−779) resulted in a slight reduction in amplitude. This suggests that although this region may not be essential, it does play a role in cell-autonomous circadian transcription. In support of this, we found potential E box–like sequences within this region.

We identified three E′-box sequences (E′1, E′2, and E′3) within the core transcription-regulatory region, *Per3* (−779 to −170), and showed that they were regulated by BMAL1-CLOCK and contributed to the circadian expression of *Per3*, as expected. A non-canonical E box has been reported to play an indispensable role in the cell-autonomous circadian transcription of another *Per* gene, *Per2* (27, 28). Interestingly, the three E′ boxes identified within the transcription-regulatory region of *Per3* have different characteristics. First, an *in silico* comparison of these E′ boxes among mammals revealed that E′1 is only found in humans. This indicates that the circadian expression of human *Per3* requires more robust regulation compared with that in other mammals, which supports the frequent reports of a genetic association between human *Per3* and circadian-related disorders. Second, E′2 and E′3 are interdependent, with the simultaneous binding of BMAL1-CLOCK to both E′ boxes required for transcriptional activation. Tandemly repeated E/E′ boxes have been reported to contribute to the amplitude and non-linearity of circadian transcription (29–32). It remains unclear why both E′2 and E′3 are required for the binding of BMAL1-CLOCK despite the fact that the core sequences in E′2 and E′1 are exactly the same. It is possible that nucleotide sequences surrounding E′ boxes may have a role in determining the different characteristics of these elements. For example, previous reports demonstrated a strong preference of circadian transcription factors for an adenine nucleotide in the flanking region of E boxes (32, 33); therefore, it is possible that the lack of a flanking adenine may be responsible for the reduced binding affinity between BMAL1-CLOCK and E′2. Further studies are required to confirm this. Third, there is strong evidence from reporter assays and bioluminescence monitoring indicating that a transcription repressor binds to E′2 independently of E′3 in the absence of BMAL1-CLOCK. Consistent with this hypothesis, an *in silico* analysis showed that inhibitory basic helix-loop-helix transcription factors were more likely to bind to E′2 and its surrounding sequences, compared with other E′ boxes. DEC1 and DEC2, inhibitory basic helix-loop-helix factors with circadian transcription repressor action, may constitute such repressors (34).

We showed that two D/D′ boxes underlie the detectable circadian transcription of *Per3* in the absence of the three E′ boxes. Importantly, access to the D/D′ boxes by DBP may be dependent on the activation state of the E′ boxes. In other words, BMAL1 and CLOCK may function to convert the transcription-regulatory region of *Per3* into an active state to enable DBP to access the D/D′ boxes and synergistically activate *Per3* transcription, leading to a drastic increase of circadian amplitude. Several lines of evidence support this hypothesis. First, overexpression of DBP alone resulted in only minor activation of *Per3* transcription, but in the presence of BMAL1 and CLOCK overexpression, it induced synergistic activation of *Per3* transcription (Fig. 3*B*). Second, loss of the two D/D′ boxes did not affect circadian robustness but resulted in a drastic decrease in circadian amplitude (Fig. 3*C*). Third, loss of the two D/D′ boxes did not affect circadian amplitude in the absence of all three E′ boxes (Fig. 4*A*).

The role of each of the three E′ boxes and two D/D′ boxes is summarized in Fig. 5*A*. The E′1, E′3, D, and D′ boxes contribute to the maintenance of circadian amplitude, whereas E′2 and E′3 activate transcription in an interdependent manner. We hypothesize that a deep circadian trough may result from the binding of a transcription repressor to E′2 in the absence of BMAL1-CLOCK; however, further studies are required to confirm this. Interestingly, loss of the E′ boxes and D/D′ boxes delays and advances the circadian phase of *Per3* transcription, respectively. The mechanisms underlying these differential

Figure 4. E′- and D/D′-box elements cooperate together to induce robust circadian oscillation of *Per3* expression. *A*, real-time monitoring of bioluminescence in U2OS cells transfected with *hPer3-luc* constructs of the indicated combinations of deleted E′- and D/D′ boxes. Representative graphs show data from three replicates from a single assay. After synchronization by dexamethasone treatment (50 nM for 2 h), bioluminescence was measured and integrated for 1 min at 15-min intervals. Bioluminescence (*y* axis) was measured in cpm. Schematic representations of the deleted E′- and D/D′-box elements (*light gray cross-marked boxes*) are indicated *above* each graph. *Light gray curves* represent the wild-type (−779 to +170) construct. *B*, relative detrended data sets obtained across a 2-day period were obtained by subtracting the 24-h simple moving average from three replicates of raw data. *Light gray curves* represent the wild-type (−779 to +170) construct, and the peak value of the first curve was set to 1. *C–E*, robustness, amplitude, and acrophase from the data set in *B* were calculated by curve fitting using the Cosinor software provided by Dr. Refinetti. Amplitude and acrophase of the wild-type (−779 to +170) construct (Fig. 2) were set to 1 and 0, respectively. Data indicate mean ± S.D. (*error bars*) ($n = 3$). *White circles* in *C* and *D* indicate individual data points from replicates. The mean values were compared with that of the wild-type D and D′ boxes (*darkest gray bars* or *circles*) within each ΔE′ group using the Dunnett's test, and *asterisks* indicate statistical significance ($p < 0.05$).

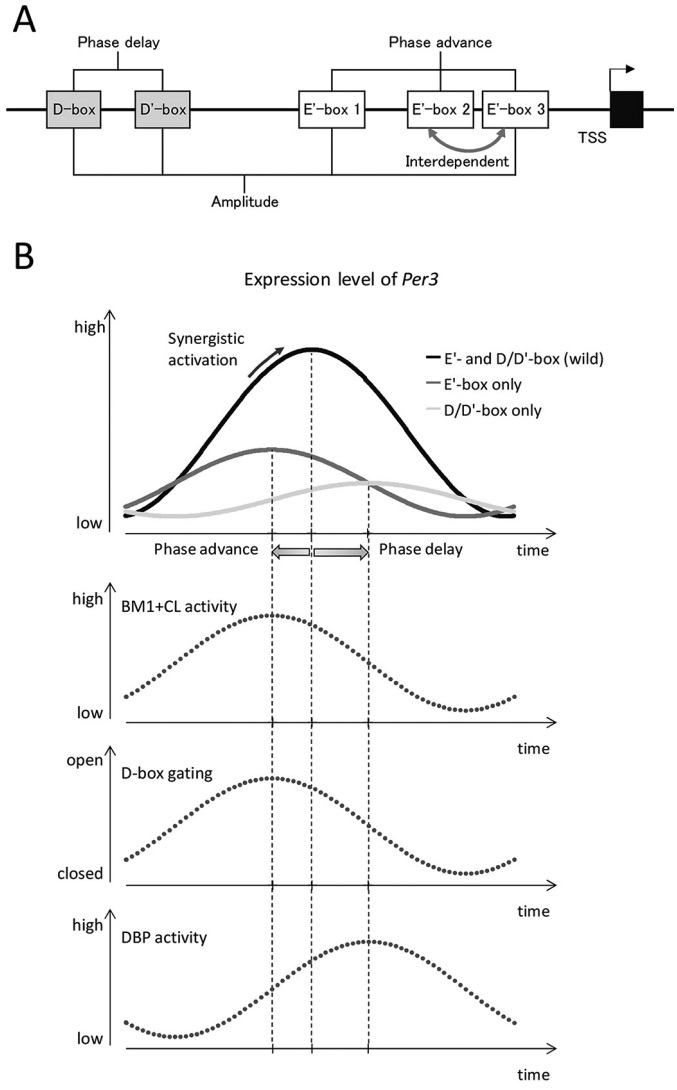

Figure 5. E′- and D/D′ boxes regulate the cell-autonomous transcriptional circadian rhythm of *Per3*. *A*, the role of each of the three E′ boxes and two D/D′ boxes. The E′1-, E′3-, D-, and D′ boxes contribute to the maintenance of circadian amplitude, whereas E′2 and E′3 activate transcription in an interdependent manner. *B*, model of phase determination by E′- and D/D′ boxes in the cell-autonomous circadian transcriptional oscillation of *Per3*. When the transcription-regulatory region of *Per3* contains only E′ boxes and no D/D′ boxes, *Per3* expression (*dark gray line*, *top panel*) is correlated with the circadian pattern of BM1 + CL (BMAL1 + CLOCK) activity (*dotted line*, *second panel*). When the regulatory region contains D/D′ boxes but no E′ boxes (*light gray line*, *top panel*) *Per3* expression is correlated with DBP activity (*dotted line*, *fourth panel*), although the circadian amplitude is low due to the limited access of DBP to the D/D′ boxes. When the transcription-regulatory region of *Per3* contains both types of transcriptional elements (*black line*, *top panel*), active BMAL1-CLOCK initiates *Per3* transcription through the E′ boxes. Accessibility of DBP to the D/D′ boxes subsequently increases following the activation of E′ boxes (*dotted line*, *third panel*), and BMAL1-CLOCK–induced DBP accelerates *Per3* transcription in a synergistic manner (*black arrow*, *top panel*).

phenotypes in circadian phase are summarized in Fig. 5*B*. When the transcription-regulatory region of *Per3* contains only E′ boxes and no D/D′ boxes, *Per3* expression is correlated with the circadian pattern of BMAL1-CLOCK activity. In contrast, when only D/D′ boxes and no E′ boxes are present, *Per3* expression is correlated with DBP activity, although the circadian amplitude is very low due to the limited access of DBP to the D/D′ boxes. The circadian phase of DBP activity is delayed compared with that of BMAL1-CLOCK activity because *Dbp* transcription is controlled by BMAL1-CLOCK (35). When the transcription-regulatory region of *Per3* contains both types of transcriptional elements, active BMAL1-CLOCK initiates *Per3* transcription through the E′ boxes. Accessibility of DBP to the D/D′ boxes subsequently increases following the activation of E′ boxes, and BMAL1-CLOCK-induced DBP accelerates *Per3* transcription in a synergistic manner. This cooperative activation of *Per3* transcription by E′- and D/D′ boxes underlies the observed enhanced amplitude and delayed phase compared with those arising due to activation of E′ boxes alone. A gradual increase in the amount of the nuclear PER-CRY complex subsequently inactivates the E′ boxes, and DBP-mediated acceleration of *Per3* transcription is simultaneously silenced even in the presence of a sufficient amount of intracellular DBP, due to limited access to the D/D′ boxes. The relative amount of *Per3* transcripts therefore begins to decrease earlier than that observed for D/D′ boxes alone. This theory may also explain the regulation of other clock genes.

Future studies should examine the potential role of surrounding nucleotides on the different characteristics of E′ boxes, identify unknown transcription repressor(s) that bind to E′2, and elucidate ways to control DBP accessibility to D/D′ boxes.

Experimental procedures

Plasmid construction

The transcription-regulatory region (−4792 to +170) of the human *Period3* gene was excised from a BAC clone (RP3-467L1) using XbaI and XhoI and subcloned into the pGL3 basic vector (Promega). Vectors containing varying lengths of *Per3* transcription-regulatory regions (from −3852/+170 to −22/+170) were constructed by digesting the excised *hPer3* sequence (−4792 to +170) with several restriction enzymes (EcoRV, KpnI, PstI, Tth111I, PmlI, BssHII, and SacI) and subsequently subcloning them into the pGL3 basic vector. The 5′- and 3′- regions of the cloned inserts were checked by sequencing. Site-directed deletion mutagenesis of *hPer3* (−779 to +170) −pGL3 was conducted according to the KOD-Plus mutagenesis kit protocol (TOYOBO, Osaka, Japan). A PCR product of the entire *hPer3* (−779 to +170) −pGL3 vector was obtained using primers designed to introduce a deletion of the target elements between their 5′ termini. After digesting the template plasmid vector with DpnI enzyme, which digests methylated DNA, self-ligation of the PCR products was performed using T4 polynucleotide kinase and ligase. The ligated plasmid DNA was transformed into competent *Escherichia coli* cells (*E. coli* DH5α competent cells; Takara, Tokyo, Japan). Plasmid DNA was purified from the transformed *E. coli* cells using an automated DNA isolation system (PI-80X, KURABO, Osaka, Japan). To check that the target elements were deleted, plasmid DNA that was digested with restriction enzymes was electrophoresed, and the consistency of band lengths was confirmed. The plasmid DNA was purified again using the QIAquick PCR purification kit (Qiagen) before transfection experiments. The mutated plasmid constructs had deletions of 4–9 base pairs overlapping the wild-type target sequences. The

mutation construct, Δ(E′2, E′3), had deletions of 18 base pairs, including the interval between E′ box 2 and 3.

For the luciferase assay and EMSA experiments, the *mBmal1*, *mClock*, and *hDbp* coding sequences were subcloned into the pcDNA3 expression vector (Invitrogen). BMAL1 and CLOCK protein were expressed as fusion proteins with c-Myc and FLAG tags, respectively.

Adenovirus vector construction

Adenoviruses carrying the luciferase gene driven by circadian promoter/enhancer elements controlling the *hBmal1*, *mPer2*, and *hPer3* clock genes were constructed as follows. The transcription-regulatory region (−4792 to +170) of the human *Period3* gene was excised from a BAC clone (RP3-467L1) using XbaI and XhoI and subcloned into the pGL3 basic vector (Promega). The resulting vector was digested using KpnI and self-ligated to produce *hPer3* (−3112 to +170) −pGL3. In addition to *hPer3*, the previously constructed vectors, *mPer2* (−2811 to +110) −pGL3 and *hBmal1* (−3465 to +57) −pGL3, were used for adenovirus vector construction (27, 36). Together with the luciferase gene, the transcription-regulatory region of these three genes was excised from each pGL3 vector, and the inserts were subcloned into the pENTR-1A vector (Thermo Fisher Scientific). The restriction enzymes used for digestion of the pGL3 vectors were as follows: *hPer3-luc*, Asp718 (KpnI) and SalI; *mPer2-luc*, Asp718 (KpnI) and SalI; *hBmal1-luc*, SalI (two restriction sites, one at the 3′-end of the SV40 late poly(A) signal sequence and one inside *hBmal1*). The resulting vectors were *hPer3* (−3112 to +170) −*luc*-pENTR-1A, *mPer2* (−2811 to +110) −*luc*-pENTR-1A, and *hBmal1* (−1683 to +57) −*luc*-pENTR-1A. These entry vectors were deposited into the RIKEN BioResource Center (RDB15084, RDB15083, and RDB15085, respectively). Before introduction into a destination vector, each pENTR-1A vector was transfected into NIH3T3 fibroblasts and synchronized by a DEX shock (50 nM), and circadian bioluminescence rhythms were confirmed by real-time monitoring with a photomultiplier tube (LM2400, Hamamatsu Photonics, Hamamatsu, Japan) in the presence of luciferin. pENTR-1A inserts were introduced into the pAd/PL-DEST vector using LR recombination. After PacI digestion, the resulting pAd/PL-DEST vectors were transfected into HEK293A cells to produce an adenoviral stock. The recombinant adenoviruses were generated using the ViraPower adenoviral gateway expression kit (K4940-00, Thermo Fisher Scientific), according to the manufacturer's instructions.

Luciferase assay

U2OS cells were cultured in 24-well plates at 37 °C with 5% CO_2 and subsequently transfected with a combination of vectors (an *hPer3-luc* reporter vector; *Renilla* luciferase vector, used as an internal control; and clock protein expression vectors). The total amount of DNA used for transfection per well was adjusted to 0.5 μg by adding empty pcDNA3. The transfection was performed using Lipofectamine 3000 and P3000 reagents (Invitrogen). After incubation for about 20 h, the cells were lysed and centrifuged at 15,000 rpm for 15 min. The supernatant (20 μl) was assayed using the Dual-Luciferase assay system (Promega). Luminescence was measured by a GloMax 20/20 luminometer (Promega). Measurement parameters were set as follows: injection volume, 100 μl; delay time after injection, 2 s; integration time, 10 s. Reported data represent firefly luciferase activity normalized to *Renilla* luciferase activity in relative light units. Dunnett's and Student's *t* test were used for comparisons. Differences were considered to be significant when the p value was <0.05.

Real-time monitoring of bioluminescence in living cells and data analysis

U2OS cells were cultured in 35-mm diameter dishes and transfected with the various mutant *Per3* promoter/enhancer-luciferase constructs using FuGENE6 (Promega). The total amount of DNA used for transfection per dish was adjusted to 1 μg by adding empty pcDNA3. After incubation for 24 h, circadian synchronization was conducted by adding DEX (final concentration 50 nM) and further incubating for 2 h. After washing the cells in DMEM (Nacalai Tesque, Kyoto, Japan), the culture medium was changed to luciferin (0.1 mM)-containing DMEM supplemented with fetal bovine serum and penicillin/streptomycin antibiotics. The bioluminescence was measured in real time and integrated for 1 min at 15-min intervals with a photomultiplier tube (LM2400, Hamamatsu Photonics, Hamamatsu, Japan). Detrended data sets were obtained by subtracting the 24-h running average from the raw data. Relative data were calculated by setting the first curve peak to 1. Circadian rhythm acrophase, amplitude, and robustness were calculated using the detrended data sets in the Cosinor software provided by Dr. Refinetti.

Adenovirus vectors expressing circadian-driven luciferase were examined according to the same procedure except that the infection was conducted by adding the adenovirus stocks ($1.24–1.47 \times 10^9$ infectious units/ml, HEK293A) to culture medium at 1:100 dilution and incubating for 1 h.

EMSA

Heterodimerized proteins of Myc-BMAL1 and FLAG-CLOCK were prepared by immunoprecipitation with FLAG antibody–conjugated beads (Sigma). HEK293A cells in 10-cm diameter dishes were co-transfected with Myc-BMAL1 and FLAG-CLOCK expression plasmids using Lipofectamine and Plus reagents (Invitrogen). Transfected HEK293A cells were lysed in 1.2 ml/dish of immunoprecipitation buffer containing 50 mM Tris-HCl (pH 8.0), 10% glycerol, 100 mM NaF, 50 mM NaCl, 2 mM EDTA, 2 mM sodium orthovanadate, 10 mM sodium pyrophosphate, 25 mM β-glycerophosphate, and 1% Nonidet P-40. Lysates was centrifuged at 15,000 rpm for 15 min. Beads were prewashed twice in immunoprecipitation buffer, and 100 μl of 50% suspended beads was added to the supernatant from cell lysate. Immunoreactions were conducted on a rotator at 4 °C for 2 h, and the beads were washed three times for 5 min. The immunoprecipitants were eluted with 200 μg/ml FLAG-peptide (Sigma). Purification was confirmed by silver staining the SDS-polyacrylamide gels using a Silver Stain MS kit (Wako, Osaka, Japan). A double-stranded oligonucleotide containing the E′-box consensus (or mutated) sequence was used as an EMSA probe. The double-stranded oligonucleotide (25 pM) was labeled with [γ-^{32}P]ATP using polynucleotide kinase

(TOYOBO, Osaka, Japan). G-50 Spin Oligo columns (GE Healthcare) were used to remove free ATP from the labeled probe. Non-radiolabeled E′-box consensus probes were used as competitors. Purified clock proteins were mixed with 0.5 nM radiolabeled probe (and competitor) in buffer containing 15 mM Tris-HCl (pH 7.5), 15 mM NaCl, 1.5 mM EDTA, 1.5 mM dithiothreitol, 7.5% glycerol, 0.3% Nonidet P-40, and 1 μg/ml BSA and incubated for 10 min. Finally, c-Myc or FLAG antibodies were added to perform supershift experiments. All reactions were incubated at 25 °C. The reactions were loaded onto 4% nondenaturing polyacrylamide gels and resolved at 150 V for 2 h at 4 °C. The gels were dried and exposed to X-ray film.

Author contributions—R. M. performed experiments, analyzed data, and wrote the manuscript. M. A. conceived and supervised the project and wrote the manuscript.

Acknowledgments—We thank Takahiro Matsuo, Miho Sato, Akihiko Okamoto, Rie Okamitsu, and Junko Sumino for expert technical assistance. We greatly appreciate the general support provided by Koichi Node (Saga University).

References

1. Schibler, U., and Sassone-Corsi, P. (2002) A web of circadian pacemakers. *Cell* **111,** 919–922
2. Rosbash, M. (1998) Why the rat-1 fibroblast should replace the SCN as the *in vitro* model of choice. *Cell* **93,** 917–919
3. Hastings, M. H., Reddy, A. B., and Maywood, E. S. (2003) A clockwork web: circadian timing in brain and periphery, in health and disease. *Nat. Rev. Neurosci.* **4,** 649–661
4. Dunlap, J. C. (1999) Molecular bases for circadian clocks. *Cell* **96,** 271–290
5. Reppert, S. M., and Weaver, D. R. (2001) Molecular analysis of mammalian circadian rhythms. *Annu. Rev. Physiol.* **63,** 647–676
6. Ko, C. H., and Takahashi, J. S. (2006) Molecular components of the mammalian circadian clock. *Hum. Mol. Genet.* **15,** R271–R277
7. Akashi, M., Okamoto, A., Tsuchiya, Y., Todo, T., Nishida, E., and Node, K. (2014) A positive role for PERIOD in mammalian circadian gene expression. *Cell Rep.* **7,** 1056–1064
8. Chiou, Y. Y., Yang, Y., Rashid, N., Ye, R., Selby, C. P., and Sancar, A. (2016) Mammalian Period represses and de-represses transcription by displacing CLOCK-BMAL1 from promoters in a Cryptochrome-dependent manner. *Proc. Natl. Acad. Sci. U.S.A.* **113,** E6072–E6079
9. Schmalen, I., Reischl, S., Wallach, T., Klemz, R., Grudziecki, A., Prabu, J. R., Benda, C., Kramer, A., and Wolf, E. (2014) Interaction of circadian clock proteins CRY1 and PER2 is modulated by zinc binding and disulfide bond formation. *Cell* **157,** 1203–1215
10. Takumi, T., Taguchi, K., Miyake, S., Sakakida, Y., Takashima, N., Matsubara, C., Maebayashi, Y., Okumura, K., Takekida, S., Yamamoto, S., Yagita, K., Yan, L., Young, M. W., and Okamura, H. (1998) A light-independent oscillatory gene mPer3 in mouse SCN and OVLT. *EMBO J.* **17,** 4753–4759
11. Zylka, M. J., Shearman, L. P., Weaver, D. R., and Reppert, S. M. (1998) Three period homologs in mammals: differential light responses in the suprachiasmatic circadian clock and oscillating transcripts outside of brain. *Neuron* **20,** 1103–1110
12. Shearman, L. P., Jin, X., Lee, C., Reppert, S. M., and Weaver, D. R. (2000) Targeted disruption of the mPer3 gene: subtle effects on circadian clock function. *Mol. Cell Biol.* **20,** 6269–6275
13. Bae, K., Jin, X., Maywood, E. S., Hastings, M. H., Reppert, S. M., and Weaver, D. R. (2001) Differential functions of mPer1, mPer2, and mPer3 in the SCN circadian clock. *Neuron* **30,** 525–536
14. Pendergast, J. S., Friday, R. C., and Yamazaki, S. (2010) Distinct functions of Period2 and Period3 in the mouse circadian system revealed by *in vitro* analysis. *PLoS One* **5,** e8552
15. Pendergast, J. S., Niswender, K. D., and Yamazaki, S. (2012) Tissue-specific function of Period3 in circadian rhythmicity. *PLoS One* **7,** e30254
16. Ebisawa, T., Uchiyama, M., Kajimura, N., Mishima, K., Kamei, Y., Katoh, M., Watanabe, T., Sekimoto, M., Shibui, K., Kim, K., Kudo, Y., Ozeki, Y., Sugishita, M., Toyoshima, R., Inoue, Y., Yamada, N., Nagase, T., Ozaki, N., Ohara, O., Ishida, N., Okawa, M., Takahashi, K., and Yamauchi, T. (2001) Association of structural polymorphisms in the human period3 gene with delayed sleep phase syndrome. *EMBO Rep.* **2,** 342–346
17. Viola, A. U., Archer, S. N., James, L. M., Groeger, J. A., Lo, J. C., Skene, D. J., von Schantz, M., and Dijk, D. J. (2007) PER3 polymorphism predicts sleep structure and waking performance. *Curr. Biol.* **17,** 613–618
18. Zhang, L., Hirano, A., Hsu, P. K., Jones, C. R., Sakai, N., Okuro, M., McMahon, T., Yamazaki, M., Xu, Y., Saigoh, N., Saigoh, K., Lin, S. T., Kaasik, K., Nishino, S., Ptáček, L. J., and Fu, Y. H. (2016) A PERIOD3 variant causes a circadian phenotype and is associated with a seasonal mood trait. *Proc. Natl. Acad. Sci. U.S.A.* **113,** E1536–E1544
19. Costa, M. J., So, A. Y., Kaasik, K., Krueger, K. C., Pillsbury, M. L., Fu, Y. H., Ptacek, L. J., Yamamoto, K. R., and Feldman, B. J. (2011) Circadian rhythm gene period 3 is an inhibitor of the adipocyte cell fate. *J. Biol. Chem.* **286,** 9063–9070
20. Bunger, M. K., Wilsbacher, L. D., Moran, S. M., Clendenin, C., Radcliffe, L. A., Hogenesch, J. B., Simon, M. C., Takahashi, J. S., and Bradfield, C. A. (2000) Mop3 is an essential component of the master circadian pacemaker in mammals. *Cell* **103,** 1009–1017
21. Koike, N., Yoo, S. H., Huang, H. C., Kumar, V., Lee, C., Kim, T. K., and Takahashi, J. S. (2012) Transcriptional architecture and chromatin landscape of the core circadian clock in mammals. *Science* **338,** 349–354
22. Ueda, H. R., Hayashi, S., Chen, W., Sano, M., Machida, M., Shigeyoshi, Y., Iino, M., and Hashimoto, S. (2005) System-level identification of transcriptional circuits underlying mammalian circadian clocks. *Nat. Genet.* **37,** 187–192
23. Nagoshi, E., Saini, C., Bauer, C., Laroche, T., Naef, F., and Schibler, U. (2004) Circadian gene expression in individual fibroblasts: cell-autonomous and self-sustained oscillators pass time to daughter cells. *Cell* **119,** 693–705
24. Balsalobre, A., Brown, S. A., Marcacci, L., Tronche, F., Kellendonk, C., Reichardt, H. M., Schütz, G., and Schibler, U. (2000) Resetting of circadian time in peripheral tissues by glucocorticoid signaling. *Science* **289,** 2344–2347
25. Matsumura, R., Okamoto, A., Node, K., and Akashi, M. (2014) Compensation for intracellular environment in expression levels of mammalian circadian clock genes. *Sci. Rep.* **4,** 4032
26. Gekakis, N., Staknis, D., Nguyen, H. B., Davis, F. C., Wilsbacher, L. D., King, D. P., Takahashi, J. S., and Weitz, C. J. (1998) Role of the CLOCK protein in the mammalian circadian mechanism. *Science* **280,** 1564–1569
27. Akashi, M., Ichise, T., Mamine, T., and Takumi, T. (2006) Molecular mechanism of cell-autonomous circadian gene expression of Period2, a crucial regulator of the mammalian circadian clock. *Mol. Biol. Cell* **17,** 555–565
28. Yoo, S. H., Ko, C. H., Lowrey, P. L., Buhr, E. D., Song, E. J., Chang, S., Yoo, O. J., Yamazaki, S., Lee, C., and Takahashi, J. S. (2005) A noncanonical E-box enhancer drives mouse Period2 circadian oscillations *in vivo*. *Proc. Natl. Acad. Sci. U.S.A.* **102,** 2608–2613
29. Nakahata, Y., Yoshida, M., Takano, A., Soma, H., Yamamoto, T., Yasuda, A., Nakatsu, T., and Takumi, T. (2008) A direct repeat of E-box-like elements is required for cell-autonomous circadian rhythm of clock genes. *BMC Mol Biol.* **9,** 1
30. Rey, G., Cesbron, F., Rougemont, J., Reinke, H., Brunner, M., and Naef, F. (2011) Genome-wide and phase-specific DNA-binding rhythms of BMAL1 control circadian output functions in mouse liver. *PLoS Biol.* **9,** e1000595
31. Tokuda, I. T., Okamoto, A., Matsumura, R., Takumi, T., and Akashi, M. (2017) Potential contribution of tandem circadian enhancers to nonlinear oscillations in clock gene expression. *Mol. Biol. Cell* **28,** 2333–2342
32. Muñoz, E., Brewer, M., and Baler, R. (2002) Circadian transcription: thinking outside the E-Box. *J. Biol. Chem.* **277,** 36009–36017

33. Hogenesch, J. B., Gu, Y. Z., Jain, S., and Bradfield, C. A. (1998) The basic-helix-loop-helix-PAS orphan MOP3 forms transcriptionally active complexes with circadian and hypoxia factors. *Proc. Natl. Acad. Sci. U.S.A.* **95,** 5474–5479
34. Honma, S., Kawamoto, T., Takagi, Y., Fujimoto, K., Sato, F., Noshiro, M., Kato, Y., and Honma, K. (2002) Dec1 and Dec2 are regulators of the mammalian molecular clock. *Nature* **419,** 841–844
35. Ripperger, J. A., and Schibler, U. (2006) Rhythmic CLOCK-BMAL1 binding to multiple E-box motifs drives circadian Dbp transcription and chromatin transitions. *Nat. Genet.* **38,** 369–374
36. Akashi, M., and Takumi, T. (2005) The orphan nuclear receptor RORα regulates circadian transcription of the mammalian core-clock Bmal1. *Nat. Struct. Mol. Biol.* **12,** 441–448